

Pair distribution function analysis for Pt-Pd-Co atomic mobility in nanoparticles

G. Hernandez, J.J. Araiza Ibarra, J.A. Vargas Téllez

Through the in-situ monitoring of fuel cells in oxidation-reduction processes with ternary nanoparticles (Pt-Pd-Co), the Pair Distribution Function (PDF) is created by the Fourier transform of the high-energy X-ray diffraction pattern of the sample. Lattice deformations in nanostructures have been shown to be reflected in the oscillation of the peaks of the atomic PDF. Analyses have revealed that there is atomic mobility within the nanoparticles. Thus, in this work we study the effect on PDF of different internal variables for nanoparticles modeled based on data from a previous interdisciplinary study by a third party, the variables include temperature, vacancies and atomic species distribution. Several atomic structural models were created, and molecular dynamics simulations were applied to them using LAMMPS and the Modified Embedded Atom Method (MEAM) for the atomic interaction. The PDF's generated from the models were compared to experimental data and the best match was identified. It is shown that a non-uniform distribution of the elements of the ternary system within the structures is the cause of the lattice strain oscillations for the nanostructures, mainly the radial distribution of Co turns out to have a greater effect on the peaks of interest in the PDF altering the general structure of the nanoparticles.

Introduction

The atomic Pair Distribution Function (PDF) is a tool that gives us a statistical description of the arrangement of atoms within a material, giving us a complete overview of the average atomic structure at short and long ranges, a fact that is invaluable in the study of amorphous materials, with low structural coherence, or for nanostructured materials, due to the significant effect their surface has on them. The PDF technique is obtained by applying a Fourier transform to the data obtained from X-ray or neutron diffraction experiments [1].

In 2021 Zhi-Peng *et al.* used the PDF to study nanoscale catalysts in an *operando* fuel cell. They monitored the oxidation-reduction process using in the cathode nanoparticles with a Pt-Pd base and 3d transition metals (Cu, Ni and Co) [2]. Other studies have found very useful the PDF analysis in conjunction with atomic models in similar operating environments [3], to evaluate the structure of the sample [4] and get a more detailed insight of the strains, defects and morphology of different nanostructures [5-8].

As a collaboration with the group who carried out the experiment with the fuel cell [2], we were provided with a PDF profile of Pt-Pd-Co nanoparticles after several cycles of operation inside the fuel cell. This PDF profile was obtained by high-energy in-situ synchrotron X-ray diffraction after 150 minutes of operation, in which the pair distribution function has evolved over time by varying the positions and intensities of the peaks, it shows that there is atomic mobility within the structure, however, there is no atomic 3D model that shows with certainty how the structure has evolved.

In the present work, different modifications are introduced in the atomic models and their effect on the PDF is evaluated to find a model able to replicate the experimental PDF in great detail. The atomic models passed through a molecular dynamics simulation as implemented in LAMMPS [9] using the second nearest-neighbor modified embedded atom method (MEAM) [10-14].

Effect of atomic distribution on the PDF

The distribution of the atoms of the nanoparticles is very important in the shape of the PDF. Based on the grouping of

atoms within the structure, we are interested in 3 main types of simple distribution (Janus, Sandwich and Core-shell). To make their analysis easier, nanoparticles of 3 nm diameter with a composition of Pt 50% and Ni 50% were modeled in order to have a significant effect caused by their different atomic radii and dispersion power.

Figure 1 shows a comparison of the PDFs calculated for the structural arrangements mentioned in the previous paragraph, the effects on the PDF are notable for each type, firstly, the PDF profiles begin to lose sharpness for approximate widths of the most structurally stable parts of the nanoparticles, this is explained by the fact that the less structurally stable part loses structural coherence when trying to conform to the atomic structure present in the area of contact with the other part, the more stable part (Pt) maintains its coherence, while the less stable part (Ni) loses it, as the concentration of the components varies, the effects also vary showing an increase in the distances of loss of coherence when the proportion of the most stable element increases, these effects are valid for Janus and Sandwich distributions.

The Core-Shell models show a lower loss of coherence compared to Janus and Sandwich models and show a high sensitivity to the structure of the atomic species that occupies more volume (usually the core, but it depends on the size), so a PDF of a nanoparticle with two atomic species in equal proportions will be more similar to the one that makes up the nucleus.

Some effects that are present in the three types of distribution are in the first case the appearance of a small peak at a distance somewhat shorter than the maximum peak,

G. Hernandez[✉], J.J. Araiza Ibarra[✉], J.A. Vargas Téllez[✉]

Unidad Académica de Física,
Universidad Autónoma de Zacatecas,
Zacatecas, Zacatecas, 98068, México

Presented at the *Nanostructures Symposium, XVII Intl. Conf. on Surfaces, Materials, and Vacuum, SMCTSM*, September 23rd to 27th, 2024. Ensenada, BC, Mexico.

Received: October 2nd, 2024.

Accepted: December 20th, 2024.

Published: December 26th, 2024.

© 2024 by the authors. Creative Commons Attribution
https://doi.org/10.47566/2024_syv37_1-241201

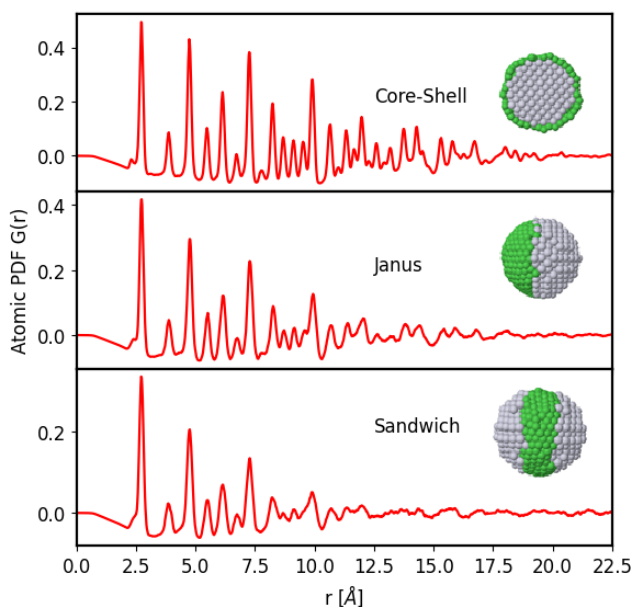


Figure 1. Comparison between atomic distribution functions for nanoparticles with Core-Shell, Janus, Sandwich atomic arrangements in proportions of Pt 50 % and Ni 50% and with size of 3 nm, in green the atoms of Ni, in white atoms of Pt, for the case Core-Shell a radial cut-off view is presented.

this small peak represents the interatomic distances for pairs of atoms with a smaller atomic radius (Ni-Ni in this case), and its intensity increases with the degree of segregation of the atomic species serving as a good indicator of the presence of Janus, Sandwich, or well-defined Core-shell structures. The second effect is that there is a small lateral shift as a function of the average atomic radius of the atomic species and their proportion, so an atomic species with a larger radius induces a rightward shift in the PDF and vice versa.

Results and discussion

The research group of Z. P. Wu *et al.* provided the average composition and size of the nanoparticles in the experiment, the characterization performed shows a size of 5 nm and a composition of 28 % Pt, 45 % Pd and 27 % Co, as well as a spherical shape, the structures were characterized by high-angle annular darkfield scanning transmission electron microscopy (HAADF-STEM) using a double-Cs corrected microscope (FEI Titan Cubed Themis Z) working at 300 kV. Sample compositions were evaluated by inductively coupled plasma optical emission spectroscopy (ICP-OES; PerkinElmer 2000 DV). The crystal structure of the samples was analyzed by X-ray diffraction (XRD) using a Phillips X'pert PW 3040 MPD diffractometer (Cu K α radiation with a wavelength of 1.5418 Å). Experiments were performed operating high-energy synchrotron X-ray diffraction (HE-XRD) with a high X-ray energy of 105.69 keV ($\lambda = 0.1173$ Å).

Early models, simulation temperature and defects

An initial approximation involved a uniform and random distribution of atomic species within the nanoparticle whose

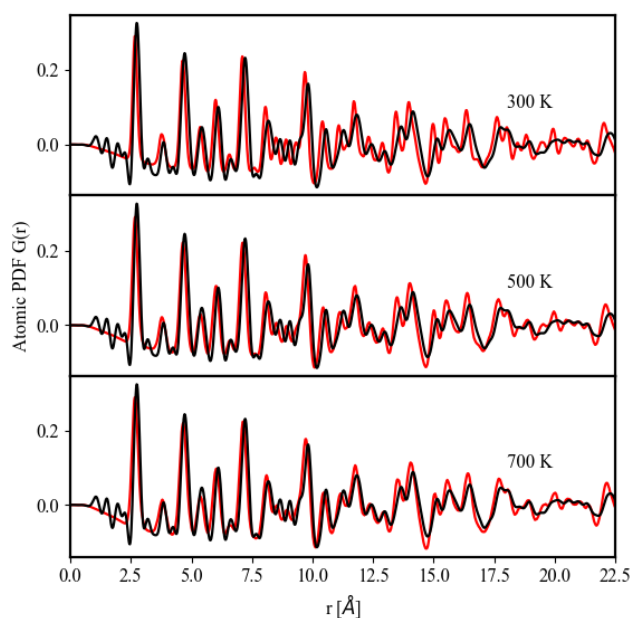


Figure 2. Comparison between the experimental PDF (black line) and simulated models for nanoparticles of 5 nm diameter (red lines) with a composition of 28 % Pt, 45 % Pd and 27 % Co, profiles obtained for simulation temperatures of 300, 500 and 700 K are shown.

only parameter of adjustment was the simulation temperature. A high simulation temperature implies a high degree of scattering of atoms over their equilibrium points, showing that the temperature rise is directly related to the loss of sharpness in the profile of the pair distribution function (Figure 2). In particular, raising the simulation temperature generates a slight outward shift of the profile

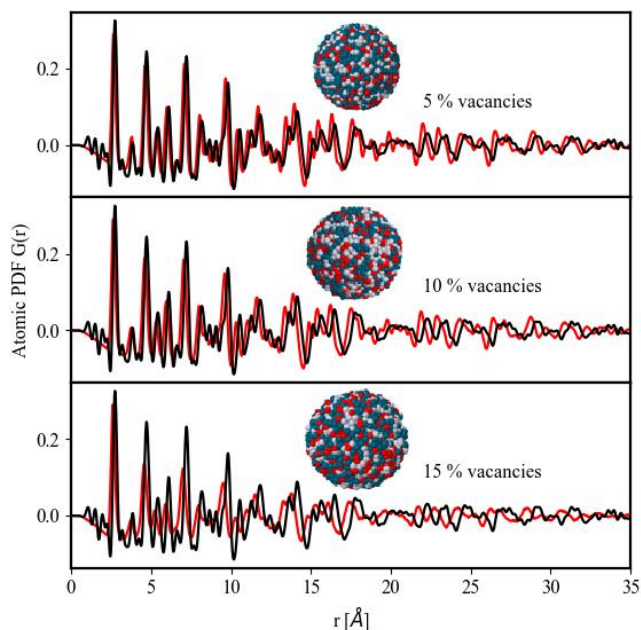


Figure 3. Comparison between PDFs of atomic models with different degrees of vacancies in the crystal lattice, have uniform distribution of atomic species (28% Pt, 45% Pd and 27% Co) and simulated at 450 K, in all cases the vacancies are atoms randomly removed along the structure before the simulation. Views are shown with the atoms of Co in red, Pt in white, and Pd in blue.

(around 0.5 Å per 200 K), an effect that can be interesting in fine-tuning with some models.

The relationship between the temperature of the simulation and the intensity of the peaks of interest is of vital importance, an adequate temperature alone is capable of drastically reducing the total error between experimental and simulated data, however, it is not enough.

Introducing vacancies in the initial lattice of a model is capable of generating interesting effects that can be useful when looking for a model that replicates an experimental pair distribution function.

The existence of vacancies in a structural model is directly related to the degree of disorder within the model, this is explained by the following process: when we have a structural model from which a certain number of atoms are randomly removed we generate empty spaces that represent alterations in the potentials in that area, by applying the simulation of molecular dynamics we cause atomic mobility in the surrounding area to fill the voids of potential, thus generating an atomic deviation of the equilibrium points of the network.

This has repercussions in the PDF (as shown in Figure 3), where it is seen that in a greater degree of vacancies there is a loss of intensity from the second peak and a greater variation of small peaks beyond the positions of the first neighbors, the loss becomes quite noticeable at distances of 3.8 and 25 Å. There is also a shift to the left of the profiles, which increases along with the percentage of vacancies, caused by a small contraction of the nanoparticle when atomic mobility occurs, and evidenced by the average interatomic distances, where for 5% of vacancies we have 24.85 Å, for 10% it is 24.70 Å, and for 15% it is 24.40 Å. Vacancies in the surface layers of nanoparticles do not have significant effects because they mainly affect the most distant peaks, which tend to have a lot of dispersion.

Although other defects may appear within the spectrum of possibilities of nanoparticle formation, they do not represent a case of interest for our study since their statistical representation is usually quite low given the nature of the experimental PDF (note that the profile obtained experimentally is the average from the entire distribution of the nanoparticles).

Non-uniform radial distribution and final adjustment

By direct comparison of the experimental data with those obtained from simulations of structures already seen, the PDF's changes shown in the previous section are insufficient. Therefore, a structure with a radial variation of Co was explored. The total concentration of Co was fixed at 27% while the relative amount of Co in the layers of the nanoparticle varies, having layers where Co is the majority, and layers without Co.

When cobalt varies radially, it is observed that the intensity of particular peaks of the PDF increases (Figure 4), together with a shift to the right with the concentration of cobalt to the outside, otherwise these behaviors are reversed.

The limit cases of radial distribution of some element (beyond those seen in Figure 4) in practice end up recreating

Core-Shell nanoparticles due to the strong segregation imposed on the elements.

By knowing the consequences of varying the radial distribution of cobalt in the models, it is possible to find a model which has the minimum error. The model showed in Figure 4a have a cobalt concentration of 8% at the core, while the concentration of cobalt per layer increases to 82% near to the surface.

The adjusted model is given with a simulation temperature of 300 K and shows a total error with magnitude of 0.34 (cumulative square difference per point up to 60 Å of calculation), resulting in less than one-fifth of the error compared to the first models. A more detailed analysis shows that this model has a lateral shift of certain peaks, the first being the most obvious, however, this shift ranges between 0.02 and 0.04 Å. The intensity of all peaks has been adjusted as much as possible (0.02 approximate average in magnitude for $G(r)$), except for the first maximum which shows a difference with a magnitude of 0.03.

The partial PDFs of the adjusted model are shown in Figure 5. The Co-Pd, Pd-Pd, Pt-Co and Pt-Pd partials are very similar to the total, while the Pt-Pt partial PDF has its

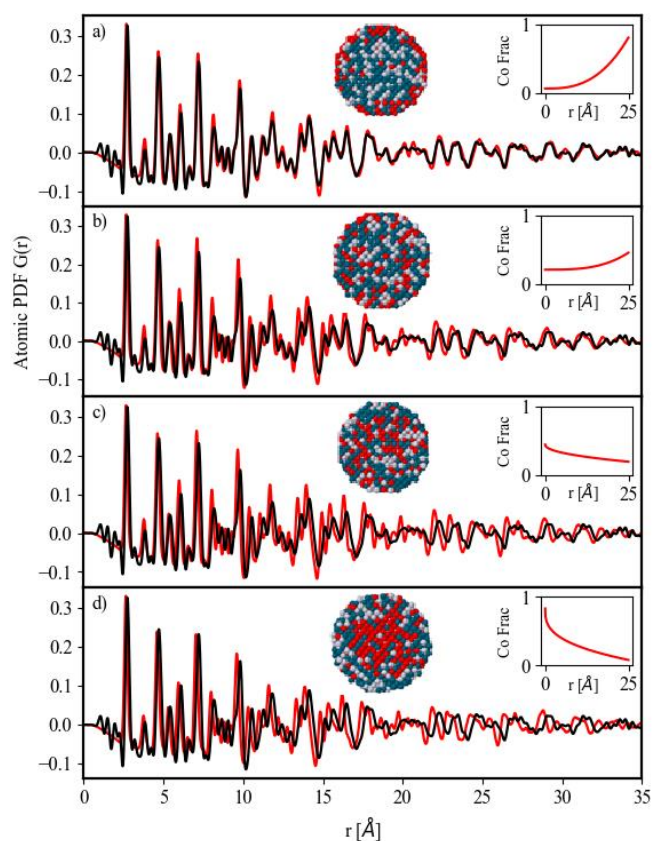


Figure 4. Comparison between PDFs obtained by varying the distribution of Co radially (red line) in contrast to the experimental (black line), the corresponding radial views are shown with the atoms of Co in red, Pt in white, and Pd in blue. In the upper right corner, the average fraction of atoms per radius. In approximate terms of relative concentration by radius a) it has 8% of Co towards the center and 82% outside, for b) 20% towards the center and 50% towards the outside, for c) 50% towards the center and 18% towards the outside, finally, d) it has 82% towards the interior and 5% towards the exterior.

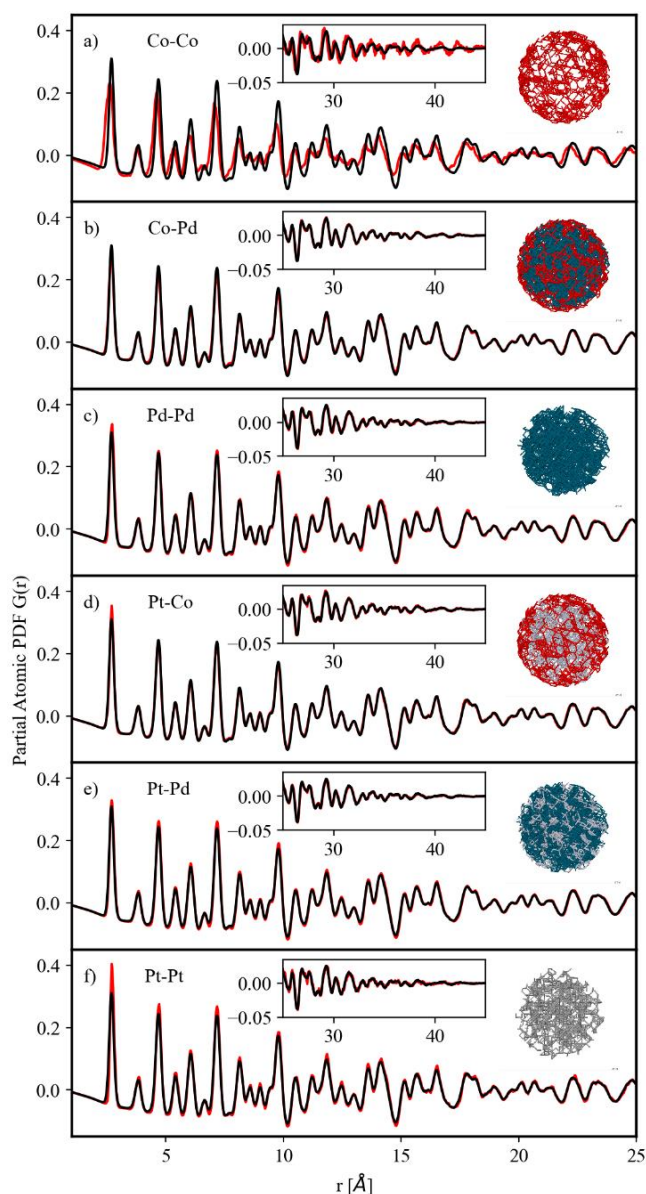


Figure 5. Comparison between partial PDFs (obtained by keeping only the referred atomic species in the model, red lines) and the total PDF of the final adjusted model (black line). 3D views of the chemical bonds are shown on the sides: Co bonds in red, Pt bonds in white, and Pd bonds in blue. In the center of the graphs, a view of the far end of the PDFs is included. The shown PDFs and the respective contributions are: a) Co-Co (3.7%), b) Co-Pd (29.7%), c) Pd-Pd (12.6%), d) Pt-Co (16.5%), e) Pt-Pd (32.8%), f) Pt-Pt (4.7%).

larger deviations in the relative height of the first important peaks. The Co-Co partial PDF exhibits the largest deviations from the total. It is clear a shift toward smaller distances and lower peak heights throughout the entire PDF, showing less structural order. However, the most interesting feature is the stronger oscillations of $G(r)$ at larger distances. This is a consequence of the Co distribution, since more Co atoms are near to the particle surface, i.e. further apart from most Co atoms.

Although the Co-Co partial PDF deviates more from the final PDF, its statistical weight is low and only relevant for the previously discussed lateral shifts (see Figure 4). The

statistical weight relates to each element's diffraction power, proportional to its number of electrons, and the number of pairs in the partial PDFs. Pt-Pd and Co-Pd have the highest statistical weights due to their high number of pairs, with Pt-Pd predominant before 30 Å and Co-Pd after 30 Å.

Conclusions

Our results show that the pair distribution function is able to provide quite detailed information about the atomic distribution within a population of nanoparticles with great precision. Similarly, the results show that PDF can be used to improve existing atomic structural models, as well as validate them.

It turned out that the atomic distribution within the nanostructures has significant effects on the PDF, and based on this it is possible to differentiate between atomic arrangements such as Janus, Sandwich, Core-Shell or a uniform arrangement. It was also shown that in a uniform distribution of elements the temperature of the simulation is not a sufficient factor to be able to adjust with the experimental data. However, it follows that desired effects can be emulated in a more refined model by changing the simulation temperature. In addition, the addition of vacancies to structural models results in structural coherence losses seen in the PDF, which can emulate materials with a high degree of atomic disorder.

In the end, it was found that a partial and continuous radial segregation of cobalt within the nanoparticles better suited the given experimental PDF, thus showing that the atomic diffusion of Co within the nanoparticle manages to reproduce what was experimentally observed. In the simulated models, it was found that a majority concentration of cobalt on the surface of the nanoparticle showed a better fit to the experiment profile.

References

- [1]. H.P. Klug, L.E. Alexander, *X-ray diffraction procedures for polycrystalline and amorphous materials* (John Wiley & Sons, 1974).
- [2]. Z.P. Wu, D.T. Caracciolo, Y. Maswadeh, J. Wen, Z. Kong, S. Shan, J.A. Vargas, S. Yan, E. Hopkins, K. Park, A. Sharma, Y. Ren, V. Petkov, L. Wang, C.J. Zhong, *Nat. Commun.* **12**, 859 (2021).
- [3]. V. Petkov, B. Prasai, S. Shan, Y. Ren, J. Wu, H. Cronk, J. Luo, C.J. Zhong, *Nanoscale* **8**, 10749 (2016).
- [4]. J.A. Vargas, V. Petkov, E.S.A. Nouh, R.K. Ramamoorthy, L.M. Lacroix, R. Poteau, G. Viau, P. Lecante, R. Arenal, *ACS nano* **12**, 9521 (2018).
- [5]. R.B. Neder, V.I. Korsunskiy, *J. Phys-Condens. Mat.* **17**, S125 (2005).
- [6]. V. Petkov, *Pair distribution functions analysis, in Characterization of Materials* (John Wiley & Sons, 2012).
- [7]. D. Olds, H.W. Wang, K. Page, *J. Appl. Crystallogr.* **48**, 1651 (2015).
- [8]. T. Proffen, S.J.L. Billinge, *J. Appl. Crystallogr.* **32**, 572 (1999).
- [9]. A.P. Thompson, H.M. Aktulga, R. Berger, D.S. Bolintineanu, W.M. Brown, S.G. Moore, T.D. Nguyen, R. Shan, M.J. Stevens, J. Tranchida, C. Trott, S.J. Plimpton, *Comput. Phys. Commun.* **271**, 108171. (2022).

- [10]. J.S. Kim, D. Seol, J. Ji, H.S. Jang, Y. Kim, B.J. Lee, [Calphad](#) **59**, 131 (2017).
- [11]. M.I. Baskes, [Mater. Chem. Phys.](#) **50**, 152 (1997).
- [12]. H.J.C. Berendsen, J.P.M. Postma, W.F. Van Gunsteren, A. DiNola, J.R. Haak, [J. Chem. Phys.](#) **81**, 3684 (1984).
- [13]. D. Frenkel, B. Smit, [Understanding molecular simulation: from algorithms to applications, 3rd Ed. \(Elsevier, 2023\)](#).
- [14]. T. Schneider, E. Stoll, [Phys. Rev. B](#) **17**, 1302 (1978).

The results included in this article were presented at the *Nanostructures Symposium, of the XVII International Conference on Surfaces, Materials, and Vacuum, SMCTSM*, September 23rd to 27th, 2024. Ensenada, BC, Mexico. (see Editorial Note https://doi.org/10.47566/2024_syv37_0-240001).

© 2024 by the authors; licensee SMCTSM, Mexico. This article is an open access article distributed under the terms and conditions of the Creative Commons Attribution license (<http://creativecommons.org/licenses/by/4.0/>).